Carbon isotopes, rare-earth elements and mercury geochemistry across the K–T transition of the Paraíba Basin, northeastern Brazil

MARIA VALBERLÂNDIA NASCIMENTO SILVA[1], ALCIDES NÓBREGA SIAL[1]*, JOSÉ ANTONIO BARBOSA[2], VALDEREZ PINTO FERREIRA[1], VIRGÍNIO HENRIQUE NEUMANN[2] & LUIZ DRUDE DE LACERDA[3]

[1]*NEG-LABISE, Department of Geology, Federal University of Pernambuco, Recife, 50670-000, Brazil*

[2]*LAGESE, Department of Geology, Federal University of Pernambuco, Recife, 50670-000, Brazil*

[3]*LABOMAR, Institute of Marine Sciences, Federal University of Ceará, Fortaleza, 60165-081, Brazil*

**Corresponding author (e-mail: sial@ufpe.br)*

Abstract: The Paraíba Basin, northeastern Brazil, is divided into three sub-basins: Olinda, Alhandra and Miriri, which encompass the formations Beberibe (Coniacian–Santonian), Itamaracá (Campanian) and Gramame and Maria Farinha (Maastrichtian to Danian, respectively). In the Olinda sub-basin, the Cretaceous–Palaeogene transition (KTB) has been recorded by the carbonates of the Gramame and Maria Farinha formations. This study focus on the behaviour of C and O isotopes, major and rare-earth elements and mercury in carbonates from three drill holes in the Olinda sub-basin. The climate was fairly cold during the marine transgression in which carbonates of the Itamaracá Formation were deposited. A temperature and bioproductivity increase has been registered in the Early Maastrichtian (Gramame Formation), with a gradual fall during the rest of this period. A positive $\delta^{13}C$ (+2‰) excursion near the KTB is followed by a drop to values around +1‰ immediately after this transition. In one drill hole, several negative $\delta^{13}C$ anomalies predate the KTB, possibly related to either multiple impacts or volcanic activity that preceded this transition. In two of the three drill holes, the total mercury increases immediately after the KTB and, in two of them, mercury spikes (four of them in one case) precede this transition, which has been interpreted as an indication that volcanic activity predated the transition. Rare earth element patterns support a marine origin for the carbonates in the Campanian–Maastrichtian transition and KTB in the Olinda sub-basin. In carbonates from one of the drill holes, absent to weakly positive Ce anomalies (−0.1 and 0.002) in the KTB coincide with a fall in $\delta^{13}C$ values, followed by an increase (from 2.3 to 1.8‰ and back to 2.3‰) and in increment in mercury values (from 0.4 to 2.7 ng g^{-1}). The presence of pyrite nodules associated with a weakly negative Eu anomaly point to slightly reducing conditions around the KTB.

The mass extinction recorded in the Cretaceous–Palaeogene transition (KTB) is generally regarded as a consequence of single (Alvarez *et al.* 1980; Claeys *et al.* 2002; Schultze *et al.* 2010) or multiple meteorite impacts, intense volcanic eruptions, or both (McLean 1978; Courtillot 1999; Hoffman *et al.* 2000; Keller 2005; Archibald *et al.* 2010) at that time.

The hypothesis of Alvarez *et al.* (1980) assumes that a single meteorite impact led to a sunlight-blocking dust cloud that killed much of the plants on Earth, reduced the global temperature, and has since been called an 'impact winter'. Their hypothesis found support in the discovery of anomalous amounts of iridium (3000 ppt), an element abundant in meteorites but rare on the Earth crust, in a 1-cm-thick clay layer in a sequence of pelagic limestones at Gubbio (Italy). Since their work was published, an increasing number of observations seem to support the impact of an extraterrestrial object at exactly the KTB: (i) the iridium anomaly detected in almost 100 sites, homogeneously distributed worldwide (Claeys *et al.* 2002), (ii) the presence of glass microspherules (Smit & Klaver 1981; Smit 1999) and shocked quartz in sedimentary rocks that registered the KTB (Bohor *et al.* 1984; Bohor 1990), and (iii) the discovery of the large Chicxulub crater in the Yucatan Peninsula, Mexico, possibly the site for the large bolide impact assumed by Alvarez *et al.* (1980).

Glass microspherules could be a result of the Chicxulub crater meteorite impact; however,

From: Bojar, A.-V., Melinte-Dobrinescu, M. C. & Smit, J. (eds) 2013. *Isotopic Studies in Cretaceous Research*. Geological Society, London, Special Publications, **382**, 85–104.
First published online May 16, 2013, http://dx.doi.org/10.1144/SP382.2

according to Stinnesbeck *et al.* (2001), this predated the KTB by 200 000 to 300 000 years. The occurrence of the Chicxulub impact crater is associated with three others (the Boltysh crater in Ukraine, dated 65.2 $\pm$ 0.6 Ma, Kelley & Gurov 2002; the Silverpit crater in the North Sea, dated 65 Ma, Stewart & Allen 2002; and the Shiva crater, India, dated *c.* 65 Ma, Chatterjee & Rudra 1996), which has led to the assumption of multiple meteorite impacts predating the KTB (Keller *et al.* 2003; Keller 2005). Strong climatic changes as a consequence of multiple meteorite impacts could be the cause of environmental stress, leading to the massive extinction of species (Keller 2001, 2005; Keller *et al.* 2003).

The hypotheses of one or multiple meteorite impacts as the main cause of mass extinction during the KTB have never reached a consensus. It is known that the largest mass extinction (the Permian–Triassic transition) coincides with the time of basaltic flows in Siberia (Campbell *et al.* 1992; Renne *et al.* 1995; Berner 2002; Beerling *et al.* 2007). Similarly, it is possible that the perturbation in the carbon cycle and the iridium anomaly in the KTB resulted from volcanism of the magnitude of the Deccan traps of west–central India (McLean 1978, 1991; Chatterjee *et al.* 2003); these gigantic eruptions formed multiple layers of solidified flood basalt (2 km thick) between 60 and 68 million years ago (Sheth 2005). The release of volcanic gases (particularly sulphur dioxide) during the formation of the traps may have contributed to contemporary climate change and acted as a major stressor on biodiversity at that time, with an average fall in temperature of 2 °C during this period (Royer *et al.* 2004). The series of eruptions (*c*. 66 Ma) near Mumbai lasted less than 30 000 years in total and perhaps can be blamed for the demise of dinosaurs. Therefore, the discovery of rapid and voluminous Deccan eruptions during the KTB suggests that iridium and other platinum group element (PGE) contributions may have been far greater than originally assumed and could account for, at least, some of the KTB iridium anomalies.

In summary, single or multiple meteorite impacts or volcanism during the KTB contributed to a greenhouse effect and global warming, acting on an already fragile ecosystem and giving a scenario of volcanic eruptions and sea-level and climatic changes (Keller 2001, 2005).

The record of the KTB in the Paraíba Basin in northeastern Brazil, the main focus of the present study, is found in a carbonate succession represented by the Maastrichtian Gramame and Danian Maria Farinha formations. Here, we examine the carbon and oxygen isotopes, major and rare-earth elements (REEs) from core samples taken from three wells drilled in the Olinda sub-basin (Fig. 1): Poty Quarry (52 m), Olinda town (62 m) and Itamaracá Island (82 m). We also analyse the concentration of mercury in samples collected from these drill holes across the KTB in an attempt to trace a potential register of volcanism during this transition.

Location and geological setting

The coastal area of the Paraíba Basin has an area of *c.* 7600 km^2 and an offshore area of *c.* 31 400 km^2, extending on the continental shelf down to the bathymetric level of 3000 m (Fig. 1). This basin was once called the Pernambuco–Paraíba Basin, and was limited by the Pernambuco shear zone and the Touros High. Mabesoone & Alheiros (1991, 1993) assumed that this basin encompassed the Olinda, Alhandra and Miriri sub-basins, located between the Pernambuco shear zone and the Mamanguape High. Barbosa (2007) and Barbosa *et al.* (2006) suggested that the marginal basin located between the eastern extremes of the Pernambuco and Patos shear zones (which border the Transversal Zone of the Borborema Province) could be named the Paraíba Basin, encompassing the three above-mentioned sub-basins (Fig. 2).

The deposition of the Paraíba Basin started with the Beberibe Formation during the Santonian–Campanian (Beurlen 1967*a*), followed by the Itamaracá (Kegel 1955), Gramame (Beurlen 1967*b*) and Maria Farinha (Beurlen 1967*a*, *b*) formations (Fig. 2). These formations were deposited on a carbonate ramp, initially defined as a homoclinal ramp with shallow sedimentary cover (Mabesoone & Alheiros 1988, 1991, 1993). However, Barbosa *et al.* (2006) considered this ramp to be a distal steepened ramp.

Itamaracá Formation

The Itamaracá Formation (Fig. 3) is a transitional stratigraphic unit formed during the continental to marine stage, represented by estuarine and coastal lagoon deposits containing marine and brackish water fossils. This formation is composed of calciferous sandstones, shales and sandy limestones with very fossiliferous siliciclastics. Phosphate-rich levels can be found towards the top of the formation and some of them have been studied by Menor (1975) and Menor *et al.* (1999) in a geochemical survey of the overlying Maastrichtian Gramame Formation using C and O isotopes. Menor *et al.* (1999) described a phosphatic layer as part of the Gramame Formation on top of the Beberibe Formation (Santonian–Campanian). However, based on biostratigraphic correlations, Souza (1998, 2006) returned to Kegel's denomination (1955),

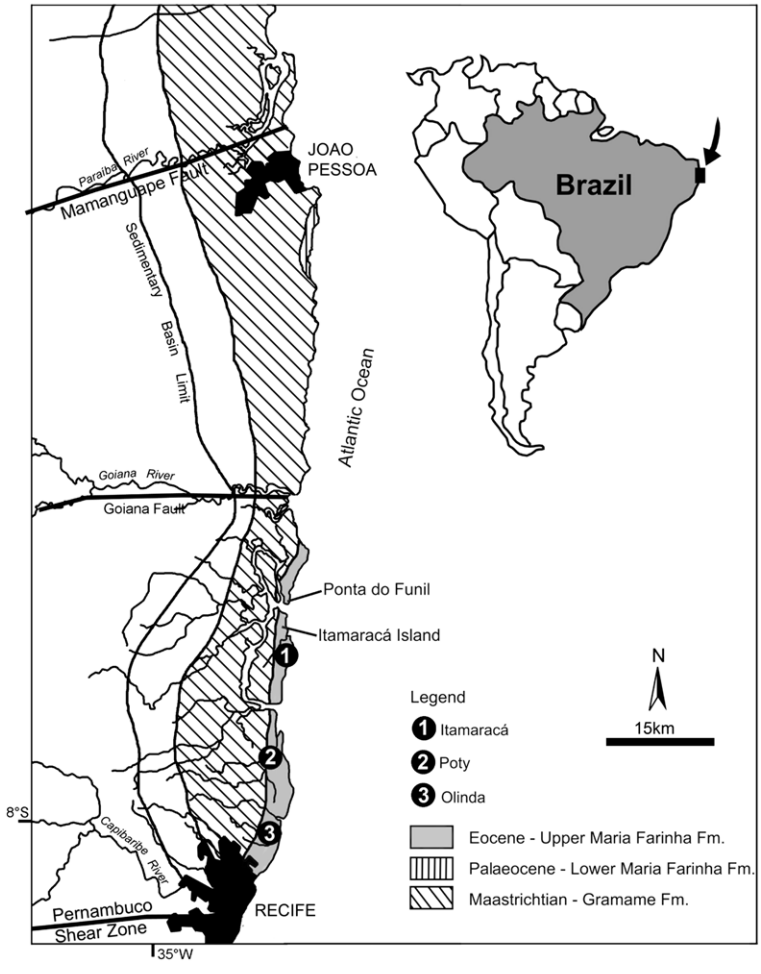

Fig. 1. The study area in northeastern Brazil, showing the location of the three sub-basins of the Paraíba Basin and the three studied drill holes: Poty Quarry, Olinda and Itamaracá. (Modified from Nascimento Silva *et al.* 2011.)

with the Itamaracá Formation interlayered between the Beberibe and Gramame formations.

The Itamaracá Formation is characterized by a maximum flood surface that contains siltic calciferous phosphatic-rich layers that separate a transgressive system tract from a highstand tract (Souza 1998, 2006; Barbosa 2007).

Gramame Formation

The Gramame Formation (Fig. 3) overlies the Itamaracá Formation and, being typical of the Maastrichtian worldwide, is composed of a limestone–marl alternation (rhythmites; Milankovitch-range to millennial-scale) deposited in a flat and shallow carbonate-mud dominated platform (Barbosa *et al.* 2006). These rhythmites act as environmental archives, directly reflecting high-frequency environmental changes (Westphal 2006). This formation displays characteristics of a high stand system tract and in its upper portion presents traces of a forced regression, just before the transition to the Palaeogene, caused or enhanced by tectonic uplift (Barbosa *et al.* 2003; Barbosa 2007).

In the Gramame Formation, microfacies are represented by biomicrites (wackestone, packstone), containing abundant microfossils (ostracodes, foraminifers, calci-spherulides) filled with spatic calcite or pyrite, detrital calcite, algae fragments, algalic mats and bioclasts disposed in micritic matrix, with very little in the way of clay minerals (Nascimento-Silva *et al.* 2011). The detrital siliciclastic content is limited, but clay minerals are abundant, probably due to the physiography of the basin, which did

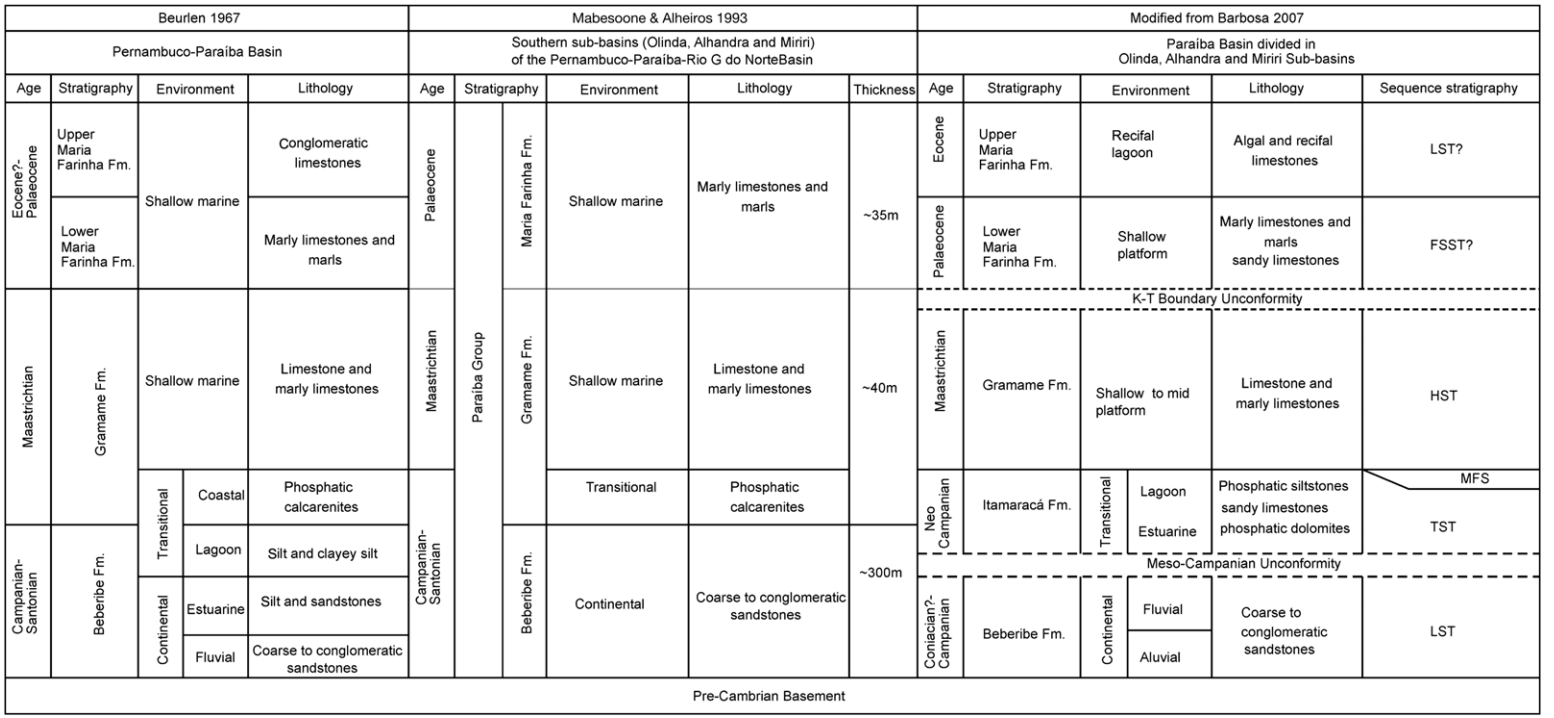

Fig. 2. Stratigraphic schemes for the Paraíba Basin, proposed by Beurlen (1967*a*, *b*), Mabesoone & Alheiros (1993) and Barbosa (2007). (Modified from Nascimento Silva *et al.* 2011.)

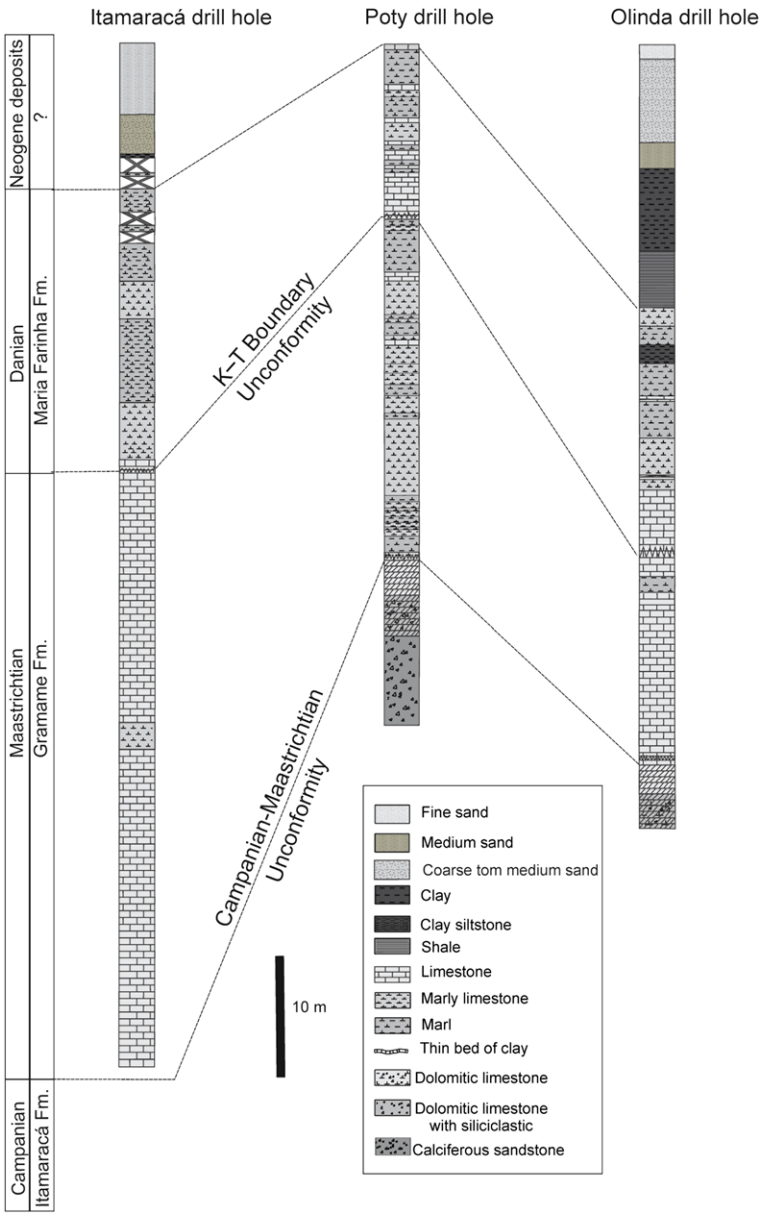

Fig. 3. Stratigraphic correlation between the drill cores of Olinda, Itamaracá and Poty Quarry. (Modified from Nascimento Silva *et al.* 2011.)

not allow sand to be transported to the platform (Barbosa *et al.* 2006; Barbosa 2007).

Maria Farinha Formation

The Maria Farinha Formation is composed of limestone, marly limestone and thick levels of marl in its lower portion (Fig. 3), while dolomitic limestone containing fossil reefs and lagunal reefs characterizes its upper portion, according to Beurlen (1967*a*, *b*). This formation exhibits the regressive characteristics of high- to low-energy oscillations (Mabesoone 1991).

At the contact between the Gramame and Maria Farinha formations there is an erosional unconformity characterized by a carbonate sequence

with intraclasts, displaying a conglomeratic aspect associated to the KTB (Albertão 1993; Albertão & Martins Jr 1996; Stinnesbeck & Keller 1996; Barbosa 2007; Barbosa *et al.* 2006). This conglomeratic layer is marked with abundant pyrite nodules (Neumann *et al.* 2009).

Microfacies are represented by biomicrites (wackestone, packstone), fossiliferous micrites (mudstone), with microfossils (foraminifers, ostracodes, calci-spheres) filled with spatic calcite or pyrite bioclasts, intraclasts and microcrystalline quartz disposed in a micritic matrix, suggesting a regression with a contribution from siliciclastic sediments. This larger concentration of siliciclastic material is the main feature in distinguishing this formation from the Gramame Formation (Nascimento-Silva *et al.* 2011).

The KTB transition in the Paraíba Basin is relatively well studied (Albertão *et al.* 1994; Stinnesbeck & Keller 1996; Koutsoukos 1998; Morgan *et al.* 2006). This record shows a preserved succession of continuous deposition across the KTB, despite an important fall in sea level during the early Palaeocene that has affected some of the KTB critical record (Stinnesbeck & Keller 1996). This event caused erosion, which has affected most of the basin and caused reworking of Lower Palaeocene and latest Upper Maastrichtian deposits (Neumann *et al.* 2009). As a consequence, the K–T transition is marked by a conglomeratic carbonate layer formed by deposits from both stages. This process has led to loss of the KTB critical layer, and we have a bed that marks the separation of the Maastrichtian and Danian (Morgan *et al.* 2006). As observed by Stinnesbeck & Keller (1996), this erosion event caused the P0 biozone loss in the first deposits of the Palaeocene, which usually contain evidence of a meteorite impact (iridium, spherules, shocked quartz) in KTB sections worldwide. However, the transition is well preserved, and studies conducted on the KTB in the Paraíba Basin have provided important results over the years.

Geochemistry

A previous geochemical study of carbonates from the Paraíba Basin examined carbon and oxygen isotopes as well as major and trace chemistry, using samples from the Poty Quarry, Olinda and Itamaracá Island drill holes (Nascimento-Silva *et al.* 2011). In that study, 165 carbonate samples from the drill core at the Poty Quarry were collected at centimetre intervals, 36 samples were collected from the Olinda drill core and 33 from the Itamaracá drill core, at 1.5 and 2.0 m intervals, respectively, and were analysed for carbon and oxygen isotopes. Twenty-five samples from the Poty Quarry drill hole were selected and analysed for carbon and oxygen isotopes, and 18 samples from the Olinda drill hole and 18 from the Itamaracá drill hole were analysed for major and trace chemistry (Tables 1–3). In the present study, this geochemical database was expanded to include REE analyses in carbonates from the Poty Quarry drill hole, as well as total mercury data from the three drill holes.

Analytical techniques

REEs from ten carbonate samples were analysed in the GEOLAB Laboratory of the GEOSOL, Belo Horizonte, Brazil. Analyses were performed with an ARL ICP 3500 with a grid of 1200 slots/mm, a Czem–Turner mounting, focal distance of 1 m, 1890 to 8000 Å scan, a linear dispersion of 8 Å/mm, a high-frequency generator (27 MHZ) with a power of 1200 W, a quartz plasma torch, an argon flux of 121/min, including pre-concentration by ion-exchange resin columns. Samples were dissolved using a tri-acid attack, comprising HF–$HCl0_4$–HCl in a Teflon crucible, followed by a dry wash to eliminate fluorine, then taken into HCl solution. Residues were separated and fused with lithium metaborate and glass formed dissolved in HCl, then added to the initial solution, which was dry washed and taken into HCl solution. In this process, pre-concentration was carried out using HCl-equilibrated cation resin. The standards used were spectroscopically pure synthetic oxides (Johnson Mattey), dissolved in HCl solution.

All of the 10 analysed samples were taken from the Poty Quarry drill hole; five were dolomitic limestones from the Campanian–Maastrichtian transition (CMT), and the other five were limestones from the limestone–marl intercalation from around the KTB.

Silica and alumina were determined by x-ray fluorescence (XRF) at the XRF Laboratory, Department of Geology, Federal University of Pernambuco, using a fused disk and the calibration curves method in a RIX-3000 Rigaku unit.

Carbon and oxygen isotopic compositions were determined at NEG-LABISE, the Federal University of Pernambuco, Brazil, using the conventional digestion method (McCrea 1950). Powdered samples were reacted with H_3PO_4 at 25 °C to release the CO_2. The $\delta^{13}C$ and $\delta^{18}O$ values were measured on cryogenically cleaned CO_2 (Craig 1957) in a triple collector SIRA II mass spectrometer. The carbon and oxygen isotopic data for the carbonatites are presented (as percent deviation with V-PDB and V-SMOW as reference, respectively). Borborema skarn calcite (BSC), calibrated against international standards, was used as the reference gas and the standard deviation of measurements was 0.15‰, in general. The values obtained for the standard

Table 1. *Geochemical composition of samples from the Itamaracá drill hole*

(**a**) Geochemical composition of the Gramame and Maria Farinha formations

Formation	Depth (m)	$\delta^{18}O$ (V-PDB‰)	$\delta^{13}C$ (V-PDB‰)	Mn/Sr	Mg/Ca	Sr (ppm)	Rb (ppm)	SiO_2 (%)	Al_2O_3 (%)
Maria Farinha	10.50	−0.94	1.21	1.55	0.81	66	143	50.06	20.94
	13.50	0.04	2.04	1.09	0.81	109	142	44.52	17.78
	18.60	0.05	1.41	1.74	0.51	81	129	43.01	21.43
	22.80	0.06	1.78	1.85	0.27	171	121	63.49	13.63
	27.00	−3.07	2.89	2.06	0.21	143	119	44.46	17.86
	31.20	−3.46	2.27	1.70	0.03	167	62	26.41	10.05
Gramame	35.10	−3.74	2.18	1.67	0.06	429	9	4.92	1.87
	37.20	−2.97	1.6	1.67	0.12	416	34	11.82	5.05
	41.40	−3.65	1.56	1.45	0.07	414	29	9.51	4.67
	45.60	−3.03	1.32	1.26	0.08	515	61	15.97	8.54
	49.80	−2.67	1.27	0.91	0.12	497	35	4.70	5.78
	54.00	−3.18	1.03	0.75	0.14	613	67	17.80	10.18
	58.20	−3.41	0.77	0.69	0.08	379	33	2.78	7.29
	62.40	−4.16	0.43	0.63	0.09	703	51	15.82	7.77
	66.60	−4.25	1.13	0.65	0.04	674	59	17.19	8.05
	70.50	−4.80	0.99	0.74	0.04	841	41	13.70	5.94
	74.70	−0.94	0.78	1.55	0.25	722	37	7.28	5.69
	78.90	0.04	1.26	1.09	0.53	760	14	9.47	2.05

(**b**) Mercury concentrations across the KTB

Formation	Depth (m)	Hg (ng g^{-1})	Lithology
Maria Farinha	32.40	2.91	Marly limestone
	32.70	2.97	Marly limestone
	33.00	3.35	Marly limestone
	33.60	4.38	Marly limestone
	33.90	3.85	Marly limestone
	34.20	1.59	Limestone
	34.50	1.06	Limestone
Gramame	34.80	0.84	Limestone
	35.10	2.60	Limestone
	35.40	1.50	Limestone

NBS-20 in a separate run against BSC yielded $\delta^{13}C$ (V-PDB) = −1.05‰ and $\delta^{18}O$ (V-PDB) = −4.22‰. These results are in close agreement with the values reported by the US National Bureau of Standards (−1.06‰ and −4.14‰, respectively).

To determine total mercury concentration, homogenized 0.25–0.5 g samples of sediments, dried at 60 °C to achieve a constant weight, were digested with an acid mixture (50% acqua regia solution), and heated at 70 °C for 1 h in a thermal-kinetic reactor 'cold finger'. Glass- and plastic-ware were decontaminated by immersion for 2 days in 10% (v/v) Extran solution (Merck), followed by immersion for three days in diluted HNO_3 (10% v/v) and final rinsing with Milli-Q water. All chemical reagents were of at least analytical grade. Cold vapor atomic fluorescence spectrophotometry (Millennium PSA2 AFS equipment) was used for mercury analysis, after Hg^{2+} reduction with $SnCl_2$. All samples were analysed in duplicate, showing reproducibility to within 9.5%. A certified reference material (NRC PACS-2, Canada) was analysed simultaneously to establish the accuracy of mercury determination. This analysis showed a precision of 4%, indicated by the relative standard deviation of the three replicates and a mercury recovery of 103 ± 4%. The mercury detection limit was estimated to be three times the standard deviation of the reagent blanks, with a value of 0.1 ng g^{-1}. In all cases, blank signals were lower than 0.5% of the sample analysis. Concentration values were not corrected for the recoveries – the amount of Hg extracted from the samples – found in the certified material.

To analyse the concentration of mercury, we studied 23 samples from limestones to marly limestones from the Poty Quarry, 10 samples from the Itamaracá drill hole and 10 from the Olinda drill hole.

Table 2. *Geochemical composition for samples from the Poty drill hole*

(**a**) Geochemical composition of the Itamaracá, Gramame and Maria Farinha formations

Formation	Depth (m)	$\delta^{18}O$ (V-PDB‰)	$\delta^{13}C$ (V-PDB‰)	Mn/Sr	Mg/Ca	Sr (ppm)	Rb (ppm)	SiO_2 (%)	Al_2O_3 (%)
Maria Farinha	7.5	−1.42	2.16	0.756	0.390	254	93	33.30	13.08
	8.7	−2.96	1.46	0.657	0.251	265	103	33.30	15.19
	9.6	−3.61	1.22	0.461	0.145	319	87	37.57	12.34
	10.2	−3.66	1.67	0.253	0.049	427	41	22.98	6.79
	11.1	−6.56	1.84	0.157	0.004	726	9	0.34	0.18
	11.7	12.17	2.33	0.378	0.269	386	77	26.78	11.99
Gramame	12.6	−4.49	1.82	0.131	0.020	533	16	10.30	3.11
	13.2	14.10	2.27	0.080	0.008	698	9	0.96	0.45
	13.8	−5.03	1.64	0.078	0.006	743	9	2.36	0.79
	15.6	−3.65	1.86	0.107	0.024	634	27	12.04	4.25
	19.2	−3.54	1.61	0.126	0.030	620	35	15.09	5.31
	25.8	−3.36	1.26	0.182	0.067	625	58	22.47	8.67
	30.6	−3.68	0.93	0.134	0.040	621	49	19.05	7.35
	36.0	−4.33	0.49	0.112	0.032	705	31	13.61	4.38
	38.4	−3.86	0.55	0.190	0.074	636	71	24.90	9.65
	42.0	−4.66	0.17	0.096	0.037	669	30	12.22	4.47
	42.3	−4.66	0.39	0.092	0.051	651	26	10.86	3.98
	43.2	−4.58	0.41	0.078	0.054	651	19	8.67	3.15
	43.8	−4.10	0.27	0.071	0.084	675	18	7.25	2.65
	44.7	−3.93	−0.27	0.082	0.101	645	16	6.13	2.27
Itamaracá	45.0	−2.68	0.36	0.098	0.206	609	15	5.98	2.27
	45.6	−2.32	−1.21	0.130	0.389	439	10	3.50	1.58
	46.2	−1.54	1.17	0.157	0.430	324	9	3.11	1.27
	46.8	−1.41	1.16	0.167	0.43	318	12	3.12	1.29
	47.4	−1.84	0.99	0.459	0.497	222	11	3.59	1.21

(**b**) Mercury concentrations of the Gramame and Maria Farinha formations

Formation	Depth (m)	Hg (ng g^{-1})	Lithology
Maria Farinha	11.4	1.37	Marl
	11.7	2.64	Marl
	12.3	0.39	Limestone
Gramame	12.6	0.73	Limestone
	12.9	0.14	Limestone
	13.2	0.13	Limestone
	13.5	0.50	Marl
	13.8	0.53	Marl
	14.1	0.18	Marly limestone
	14.4	0.46	Marl
	17.1	0.16	Marl
	17.4	0.27	Marl
	17.7	0.42	Marl
	20.1	0.12	Marly limestone
	20.4	0.28	Marly limestone
	20.7	0.25	Marly limestone
	22.2	0.43	Marl
	22.5	0.17	Marl
	22.8	0.38	Marl
	27.6	0.48	Marl
	27.9	0.56	Marl
	28.2	0.46	Marl

(**c**) Y, Th and REE concentrations across the KTB and CMT (ppm) and Ce anomaly values. Ce anomaly calculation according to Wright *et al.* (1987)

Formation	Depth (m)	Y	Th	La	Ce	Pr	Nd	Sm	Eu	Gd	Tb	Dy	Ho	Er	Tm	Yb	Lu	Ce_{anom}	Lithology
Maria Farinha	10.20	13	9	33	71	7	27	4	1	4	<1	2	<1	1	<1	1	<1	0.002	Marl
	10.80	7	5	18	32	3	12	2	<1	2	<1	1	<1	1	<1	1	<1	−0.05	Marly limestone
	11.10	3	1	4	6	1	2	1	<1	<1	<1	<1	<1	<1	<1	<1	<1	−0.12	Limestone
	11.40	15	8	39	62	7	25	4	1	4	1	3	1	2	<1	1	<1	−0.09	Limestone
	11.70	18	15	45	80	9	31	5	1	5	1	3	1	2	<1	2	<1	−0.06	Marl
Gramame Itamaracá	44.70	103	6	75	75	13	54	10	2	12	2	9	2	6	1	5	1	−0.31	Dolomitic limestone
	45.00	148	7	118	108	19	78	14	3	17	2	14	3	9	1	8	1	−0.34	Dolomitic limestone
	45.30	128	6	97	90	16	67	12	3	15	2	12	3	8	1	7	1	−0.34	Dolomitic limestone
	45.60	142	6	100	93	17	67	12	3	15	2	13	3	8	1	7	1	−0.33	Dolomitic limestone
	45.90	90	4	64	64	11	45	8	2	10	1	8	2	5	1	5	1	−0.31	Dolomitic limestone

Table 3. *Geochemical composition for sample from the Olinda drill hole*

(**a**) Geochemical composition of the Itamaracá, Gramame and Maria Farinha formations

Formation	Depth (m)	$\delta^{18}O$ (V-PDB‰)	$\delta^{13}C$ (V-PDB‰)	Mn/Sr	Mg/Ca	Sr (ppm)	Rb (ppm)	SiO_2 (%)	Al_2O_3 (%)
Maria Farinha	21.90	−0.98	1.21	1.20	0.44	226	35	20.18	4.70
	24.00	−0.46	2.04	0.73	0.55	159	127	50.16	15.30
	27.00	−1.44	1.41	0.92	0.55	152	114	44.19	15.50
	30.30	−0.78	1.78	1.13	0.68	96	147	50.41	20.20
	34.50	0.14	2.89	0.81	0.51	200	39	8.75	6.04
	36.60	−4.8	2.27	0.12	0.02	581	2	0.10	0.01
Gramame	38.70	−3.43	2.18	16.4	0.04	307	2	1.74	0.88
	40.80	−4.06	1.6	0.14	0.04	555	21	7.47	2.72
	42.90	−3.16	1.56	0.27	0.08	457	42	9.69	6.21
	45.00	−3.27	1.32	0.29	0.09	475	61	16.68	8.98
	47.10	12.83	1.27	0.27	0.07	456	41	11.91	6.55
	49.20	−3.17	1.03	0.25	0.05	467	43	13.50	6.09
	51.30	−3.86	0.77	0.20	0.05	542	42	13.59	7.23
	53.40	−4.36	0.43	0.15	0.06	624	45	14.11	6.62
	55.50	−1.66	1.13	1.01	0.37	123	52	0.57	6.11
	57.30	−1.24	0.99	0.62	0.53	162	38	4.86	5.89
	59.40	−1.17	0.78	0.34	0.47	294	16	0.97	2.47
	61.50	−0.19	1.26	0.39	0.54	217	14	1.73	1.79

(**b**) Mercury concentrations across the KTB

Formation	Depth (m)	Hg (ng g^{-1})	Lithology
Maria Farinha	36.30	2.1	Marly limestone
	36.60	1.2	Marly limestone
	36.90	2.3	Marly limestone
	37.20	2.2	Limestone
	37.50	2.2	Limestone
	38.10	1.7	Limestone
	38.40	4.5	Limestone
Gramame	39.00	2.3	Limestone
	39.60	8.9	Limestone
	39.90	11.5	Limestone

Carbon and oxygen isotopes

Stratigraphic profiles of carbon and oxygen isotopes from the drill holes at the Poty, Itamaracá and Olinda localities of the Olinda Sub-basin are shown in Figure 4. The $\delta^{18}O$ values vary from -0.9 to -1.5‰ V-PDB for the Campanian Itamaracá Formation, tending to lower values at the end of this period (-2.7‰ V-PDB), leading to the assumption that a relatively cooler climate may have prevailed. The CMT is marked by a negative excursion, which suggests a temperature increase, with values of -4 to -4.8‰ V-PDB (Fig. 4).

The values of $\delta^{13}C$ vary from $+1$ to $+1.5$‰ and suggest some organic productivity. In the CMT, values fell to -1.2‰ (Poty drill hole), but were approximately constant at the Olinda drill hole (Fig. 4).

During the Maastrichtian, carbonates of the Gramame Formation registered $\delta^{18}O$ values close to -1 and -4‰ V-PDB, with a positive trend (values closer to 0‰) and gradual fall in temperature during this interval. In the Cretaceous–Palaeogene transition, $\delta^{18}O$ values fell to -6.6‰ V-PDB, suggesting a warming of the climate (Fig. 4), followed by a sudden fall in temperature as $\delta^{18}O$ values fell to 0.1‰ V-PDB. Values from $+0.14$ to -2‰ V-PDB follow this transition, with a trend to values close to 0‰ V-PDB. In the beginning of the Maastrichtian, there was an important decrease in $\delta^{13}C$ values ($+0.03$ to 0.15‰). During the Maastrichtian, a positive trend is observed (Fig. 4), reaching values up to $+2.3$‰, which were maintained during the Cretaceous–Palaeogene transition. There is a perturbation in the $\delta^{13}C$ values in the late Maastrichtian, with values alternating between $+0.8$ and $+2.9$‰. These values are associated with the 1-m-thick conglomeratic limestone critical layer, a proxy of the erosional event that reworked the KTB sedimentary record recognized by Stinnesbeck & Keller (1996).

Silica and alumina

In samples above the CMT, after a maximum flood surface that marks the upper limit of a transgressive system tract (Souza 2006) one observes, although with some oscillation, a substantial increase in SiO_2 (up to 24.9%) and Al_2O_3 (up to 9.65%) values (Tables 2 & 3). This reflects the inflow of clay minerals into the basin.

In the Maastrichtian section at the Itamaracá drill hole, SiO_2 values reach up to 10% and Al_2O_3 up to

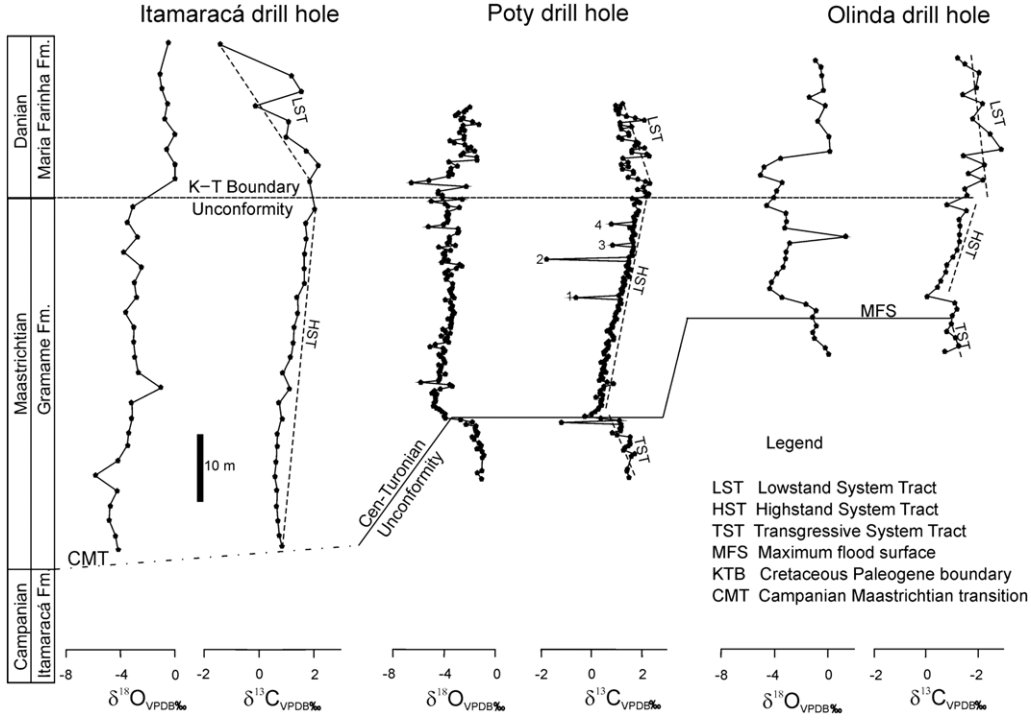

Fig. 4. Correlation among the C- and O-isotope stratigraphic profiles for the three drill holes (Olinda, Poty Quarry and Itamaracá). (Modified from Nascimento Silva *et al.* 2011.)

5%, attesting to this having the least continental influence of the three drill holes studied, with deposition of thick carbonate layers. This reflects the location of this drill hole in an open marine environment, more distal in relation to the other two drill holes (during the highstand). The limestone–marl intercalation (rhythmite) that characterizes this formation and indicates short-term climatic fluctuation is reflected in the carbon and oxygen isotope stratigraphic curves. The carbon isotope curve also exhibits a gradually increasing trend for the $\delta^{13}C$ values.

In the KTB a significant decrease in SiO_2 and Al_2O_3 can be observed, with values of up to 0.1% and 0.01%, respectively. This is observed predominantly in the drill hole at Olinda, located on the border of the Paraíba Basin. In the Poty and Itamaracá drill holes, these changes are less pronounced. This has been interpreted by Stinnesbeck & Keller (1996) as a rapid fluctuation in sea-level rise, after an erosive event resulting from a fall in sea level, immediately after the K–T event.

Above the KTB there is a substantial increase in SiO_2 and Al_2O_3 (60.5% and 21.43%, respectively). This increase corresponds to the regressive effects that took place after the end of the Maastrichtian, which are recorded in the three drill holes under consideration. In the Maria Farinha Formation, one observes the intercalation of marly layers with K-feldspar, microcrystalline quartz, clay minerals and a little carbonate, with layers composed of micritic carbonate matrix mixed with detrital minerals.

Mercury geochemistry

Volcanic eruptions are the main source of mercury injection in the environment, besides mercury of anthropogenic origin (Kot *et al.* 1999; Marins *et al.* 2004; Lacerda & Marins 2006). Volcanic emissions are an important source of mercury in the atmosphere and can cause global and regional changes in the mercury cycle (Ferrara *et al.* 2000).

Detailed mercury chemostratigraphy has been used to investigate the volcanic origin of mercury and CO_2 of carbonates deposited in the aftermath of Neoproterozoic glaciations (cap dolostones; Sial *et al.* 2010). As volcanism is supposedly one of the main causes of dramatic environmental changes during the KTB, mercury can potentially be used as a tracer of the volcanism concomitant to this transition.

With this in mind, mercury concentration was determined in a total of 42 carbonate samples from the three drill holes under consideration. These samples were collected stratigraphically from core bits of the Poty, Itamaracá and Olinda drill holes, while assuming that carbonate samples collected in this way would probably have escaped anthropogenic contamination.

The collected samples are from interlayered limestone, marly limestone and marl. In all three drill holes, mercury enrichment is mainly observed in marly layers, suggesting that the enrichment is related to the presence of clays (Tables 1–3). According to Roos-Barraclough *et al.* (2002), the association of higher contents of mercury in carbonates finely interlayered with terrigenous sediments suggests that higher mercury atmospheric deposition, originating from volcanism, resulted in higher leaching from land surface and accumulation along argillaceous carbonates, similar to the processes described in the Swiss Jura Mountains for quaternary sediments.

At the Itamaracá drill hole, mercury values around 2.6 ng g^{-1} are observed just before the KTB, followed by a fall to values around 0.84 ng g^{-1} and an enrichment to 4.38 ng g^{-1} immediately above the KTB (Fig. 5). At the Poty drill hole, mercury values increase at the KTB, and some positive mercury spikes are also present in Maastrichtian carbonate samples. There is a correspondence between the four negative spikes in the $\delta^{13}C$ stratigraphic curve and the four small increases in mercury content (Fig. 6) before the KTB. Late Maastrichtian carbonates display mercury contents from 0.12 to 0.17 ng g^{-1} with peaks around 0.5 ng g^{-1} associated with changes in the carbon cycle and in temperature. In the KTB, mercury contents reach 2.64 ng g^{-1}, where, coincidentally, there is a temperature rise for a $\delta^{18}O$ around $-2‰$ V-PDB, followed by values around $-7.5‰$ V-PDB (Fig. 6). This mercury enrichment may have resulted from significant volcanism coeval to the KTB (e.g. from nearby or from the giant Deccan basaltic volcanism in India).

Alternatively, if multiple meteorite impacts predated the KTB and caused abrupt changes in the carbon cycle, generating the four abovementioned $\delta^{13}C$ negative spikes, they could also be held responsible for small spikes in the mercury stratigraphic curve (Fig. 6).

In samples from the Olinda drill hole, mercury values between 9 and 12 ng g^{-1} can be observed before the KTB, falling to 2.3 ng g^{-1} in the KTB, with enrichment to 4.5 ng g^{-1} immediately after this transition, suggesting the possibility of volcanism preceding or coeval to the KTB (Fig. 7).

Sial *et al.* (2010) have reported mercury concentrations in carbonates from Punta Rocallosa (Chile), the deposition of which was coeval to volcanic activity, and in some carbonates from the Yacoraite Formation (Argentina), collected from about the KTB. Samples deposited during volcanic activities exhibited values from 23 to 73 ng g^{-1}, and those from about the KTB have demonstrated

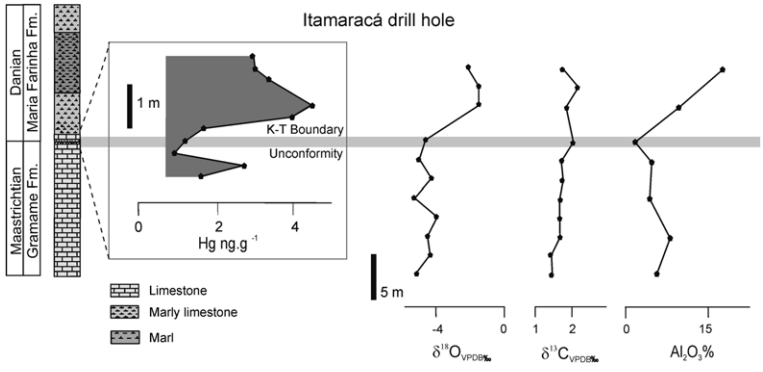

Fig. 5. $\delta^{13}C$, $\delta^{18}O$, Al_2O_3 vs. mercury stratigraphy in the Itamaracá drill hole, showing a prominent mercury anomaly in the KTB.

values between 1.5 and 6 ng g^{-1}. Those authors proposed a mercury background of <1 ng g^{-1} in sedimentary and igneous carbonates.

Similarly, in the register of the KTB of the Yacoraite Basin, carbonates from the Paraíba Basin present some mercury values >3 ng g^{-1}. The highest mercury values in carbonate samples from this basin (12 ng g^{-1}; Fig. 7) could be associated with coeval volcanism.

Sial *et al.* (1981) attempted to date Cenozoic olivine-to-alkaline basalt plugs and necks from the states of Rio Grande do Norte and Paraíba, using the K–Ar method. Although some of these basalts have proved to be younger (through Ar/Ar dating; Knesel *et al.* 2011) than previously thought, this basaltic province is centred in an area geographically close to the Paraíba Basin and perhaps active during a time interval that brackets the KTB (ages of 80.4 $\pm$ 2 Ma and 56.9 $\pm$ 1 Ma have been reported in Sial *et al.* 1981). It may therefore have been one of the sources of the somewhat high mercury concentration observed in this transition in the Paraíba Basin. Alternatively, mercury enrichment may have resulted from volcanism within the Paraíba Basin. Indeed, seismic evidence favours the presence of volcanic rocks offshore within the Paraíba Basin (Almeida *et al.* 1996).

REE geochemistry

Carbonate rocks retain the characteristics of the water from which they have been deposited, including trace elements. This means that the REE characteristics in limestones can reflect the environment in which these rocks have been formed, including depth, salinity, oxygenation levels, inflow of aerial or river-transported continental material, as well as hydrothermal contributions (Elderfield & Greaves 1982; Holser 1997; Nothdurft *et al.* 2004; Frimmel 2009, 2010).

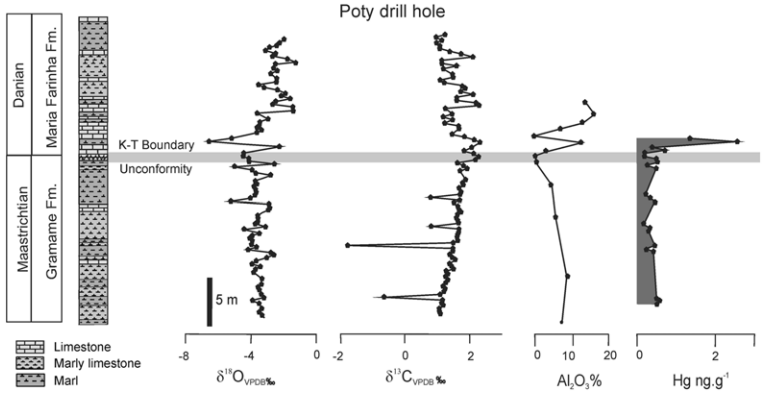

Fig. 6. $\delta^{13}C$, $\delta^{18}O$, Al_2O_3 vs. mercury stratigraphy in the Poty Quarry drill hole, showing a prominent mercury anomaly in the KTB.

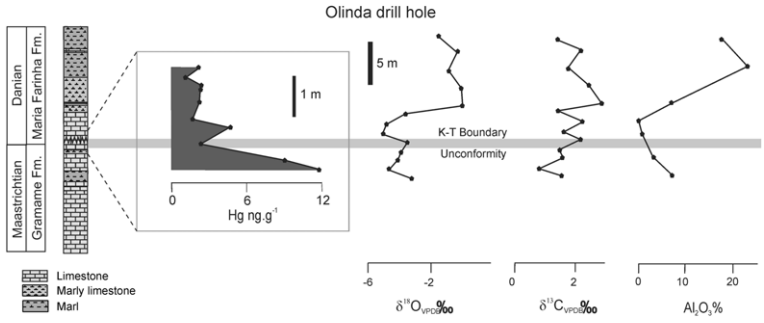

Fig. 7. $\delta^{13}C$, $\delta^{18}O$, Al_2O_3 vs. mercury stratigraphy in the Olinda drill hole, showing a prominent mercury anomaly in the KTB.

In particular, Ce and Eu anomalies have been of great use in palaeoenvironmental reconstruction. A Ce negative anomaly in sedimentary rocks, especially carbonates, has often been used as an indication of marine origin, while its absence points to the influence of continental waters (Fleet 1984; Wilde *et al.* 1996; Holser 1997; Jiedong *et al.* 1999; Frimmel 2009, 2010).

A large number of observations suggest that Ce removal from seawater is more frequent in open sea than in an estuarine environment or shelf water. Martin *et al.* (1976), when studying the Gironde estuary, verified that the Ce/La ratio remains constant, indicating that Ce is not removed in solution in estuarine environments. Water samples from the Barents Sea analysed by Hogdahl *et al.* (1968) exhibit no Ce anomaly, and nearshore waters from the east coast of the USA are 10–100 times richer in Ce than water samples from the adjacent Atlantic Ocean. Deep-sea cherts also display negative Ce anomalies, but cherts formed in extensive shelves lack such an anomaly. This suggests that Ce is depleted in open ocean waters but not in shallow sea waters (Shimizu & Masuda 1977).

Together, these considerations lead to the assumption that positive Ce anomalies in marine carbonate sedimentary rocks can indicate the presence of estuarine or coastal marine environments exposed to the influence of continental waters.

Ce anomalies can also be related to ion state changes of this element as a function of oxidation state, as observed by Elderfield & Greaves (1982). This fact was drawn from the diverging behaviour of REEs at different depths. At depths less than 100 m, one observes a Eu negative anomaly without a Ce anomaly, as well as heavy REE (HREE) enrichment in relation to light REE (LREE). At depths greater than 100 m, one observes negative Ce and Eu anomalies. Regarding the oxidation state, one observes that Ce fractionation in relation to other REEs is tied to its easier removal in the presence of oxygen. In oceans, Ce^{3+} is oxidized to insoluble Ce^{4+}, which precipitates as CeO_2, causing depletion of this element in seawater in relation to other REEs (Goldberg 1961).

The Ce anomaly can therefore be used as an indicator of eustatic variations in sea level. Positive Ce anomalies indicate oxidized conditions during falls in sea level, whereas negative anomalies are related to transgression periods, when a rise in sea level leads to deeper water and anoxic conditions. Therefore, Ce anomalies can be used as a chemical parameter in the characterization of palaeo-oceanographic conditions related to relative changes in sea level (Wilde *et al.* 1996).

An overview of factors controlling Ce anomalies in water and marine sedimentary rocks reveals that the absence of a Ce negative anomaly in carbonates does not occur with diagenetic influence, including dolomitization (Banner *et al.* 1988), but it does occur when rocks are formed in water without Ce depletion, indicating estuarine or coastal environments subjected to continental water influence (Fleet 1984). Frimmel (2009) observed systematic differences in REE + Y patterns in dolomitized and non-dolomitized samples, but without a clear relationship between the degree of dolomitization and REE abundance. Moreover, Banner *et al.* (1988) found that dolomitization of Mississippian limestones did not significantly affect their REE signatures.

Campanian–Maastrichtian Transition (CMT). The CMT in this basin is marked by a transgression event, with a decrease in continental influence and the register of a maximum flood, with deposition of a phosphatic layer (Barbosa 2007).

REEs were analysed in five dolomitic limestones samples within an interval (less of 2 m) bracketing the CMT in this basin at the Poty Quarry drill hole. These samples display North American shale composite (NASC)-normalized REE patterns that

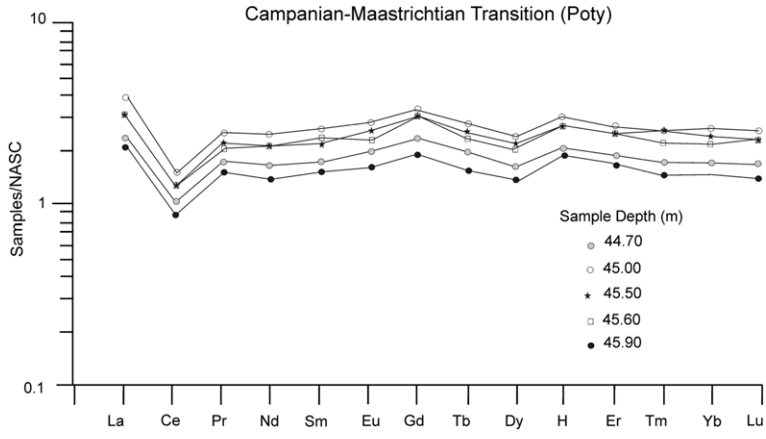

Fig. 8. NASC-normalized REE patterns (normalizing NASC values are from Haskin *et al.* 1968) for the CMT from the Poty Quarry drill hole.

are two to three times enriched in relation to NASC values (Fig. 8), with a negative Ce anomaly and almost no significant fractionation between LREE and HREE.

A negative Ce anomaly is found in ocean waters during periods of climatic warming and transgressive conditions (Wilde *et al.* 1996), and is also associated with a preferential incorporation of Ce^{4+} in authigenic minerals such as Mn nodules and phosphorites (Piper 1974; McLennan 1989). In the studied carbonates, it became clear that higher concentrations of P_2O_5 (5.3–5.6%) imply higher concentrations of REE and a more pronounced negative Ce anomaly (*c.* −0.34), and also reflect transgressive conditions and an oxidizing marine environment (Table 2).

In summary, the studied CMT carbonates in this basin with a negative Ce anomaly were formed in a reducing marine environment, during a transgression event with minor or no influence of continental water.

Cretaceous–Palaeogene Transition (KTB). Carbonate deposition during the KTB in the Paraíba Basin is marked by the end of a highstand tract system, giving way to a regressive stage.

Highstand conditions in the middle and Upper Maastrichtian sea-level fall allowed oxic conditions, generating positive Ce anomalies (Wilde *et al.* 1996). Four of the five studied carbonate samples (marl to limestone) bracketing the KTB in this basin display NASC-normalized patterns with discrete fractionation, LREE slightly higher than HREE, and patterns that are 0.1–1 times NASC values (Fig. 9). These patterns display barely negative to absent Ce anomalies, with values around −0.1, and just one marl sample shows a value of 0.002 (Table 2). Values of the Ce anomaly close to zero (> −0.10) reflect the anoxic conditions of the sea water (Wright *et al.* 1987).

The absence of negative Ce anomalies in samples from the KTB in Blake Nose, Agost and Caravaca was interpreted as in indication of a significantly low water–rock diagenetic system, and thus similar patterns to those of the precursor materials. In Blake Nose, this absence indicates no contribution from the sea water to the REE patterns, therefore preserving the characteristics of the precursor materials (spherules) (Martínez-Ruiz *et al.* 2006).

Holser (1997) correlated the behaviour of Ce during conditions of anoxia and extinction events and observed a weak positive Ce anomaly associated with Ir and $\delta^{13}C$ anomalies (Liu *et al.* 1988). In the studied samples from the Poty Quarry drill hole, absent to weakly positive Ce anomalies (−0.1–0.002) coincide with a decrease then an increase in $\delta^{13}C$ values (from 2.3 to 1.8‰ and back to 2.3‰) and an increase in mercury values (from 0.4 to 2.7 ng g^{-1}; Table 2).

The Eu behaviour also points to an environment with anoxic conditions. NASC-normalized patterns exhibit discrete fractionation with weak enrichment in LREE in relation to HREE and a discrete Eu depletion (Fig. 9). Usually, a negative Eu anomaly is observed in reducing environments, where Eu^{3+} is reduced to Eu^{2+} (Michard *et al.* 1983).

In the Agost section in Spain, where one has a record of the KTB, positive Eu anomalies have been observed in the sedimentary rocks that record this boundary (Martizez-Ruiz *et al.* 1999). These authors suggested that the observed positive Eu anomaly resulted from the highly reducing nature of the depositional environment, probably

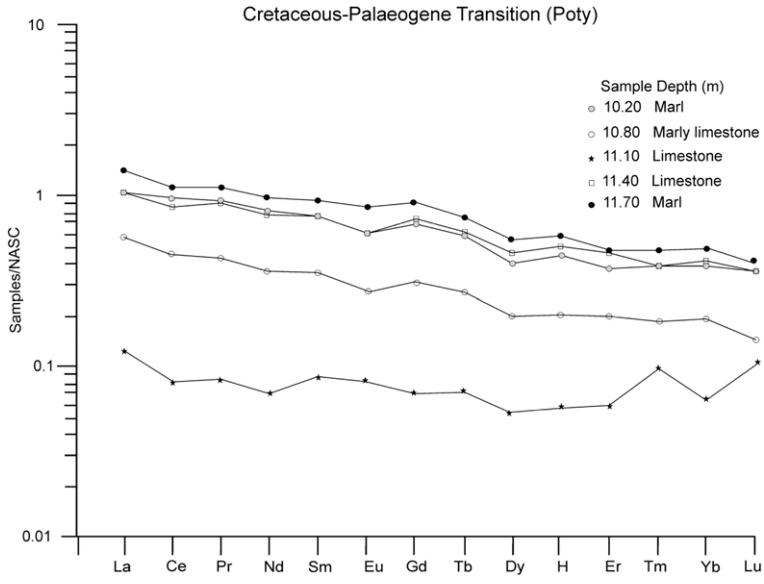

Fig. 9. NASC-normalized REE patterns (normalizing NASC values are from Haskin *et al.* 1968) for the KTB from the Poty Quarry drill hole.

developed in an ocean with minimal oxygenation and syndiagenesis conditions. This statement could be corroborated by high U concentrations and pyrite formation during the diagenesis.

The KTB in the Paraíba Basin is marked by the presence of pyrite nodules (Neumann *et al.* 2009), a proxy for a reducing environment. Pyrite has been found in large quantities in the Agost section, probably related to large amounts of organic matter deposited in the bottom of the ocean following an extinction event (Martínez-Ruiz *et al.* 1999).

In the Paraíba Basin, NASC-normalized REE patterns exhibit a discrete fractionation, with weak enrichment in LREE in relation to HREE in the KTB (Fig. 9). There is a clear influence of terrigenous material in the total REE concentrations in marl samples, which demonstrate higher REE abundances than pure limestones. This is also reflected in the weak tendency for LREE enrichment in these rocks.

Turner & Whitfield (1979) suggest that LREE are incorporated preferentially to HREE in biogenic material. Spirn (1965 in Fleet 1984) suggests that LREE are preferentially incorporated in *Globigerina* in relation to HREE, while other biogenic materials present REE concentrations 10–100 times lower than *Globigerina*. In thin sections of carbonates from the three drill holes in the Paraíba Basin, one observes a marked presence of calci-sphere foraminifera and globigerinoids. This perhaps contributed to a slight LREE enrichment in these NASC-normalized REE patterns.

Discussion

Marine carbonates have carbon isotope signatures influenced by the depositional environment. An open marine environment can exhibit an isotopic composition that differs from that of a restricted marine one, or a coastal environment with the influence of continental water (Frimmel 2010). Frimmel (2010) studied different Neoproterozoic carbonate formations and concluded that carbon isotopes cannot be used by themselves as markers for global correlation, because they record peculiarities of the depositional environment. Positive $\delta^{13}C$ excursions can result from an increase in bioproductiviy and/or an increase in evaporation in shallow marine, coastal or temporarily restricted environments. Phanerozoic carbonates usually exhibit primary carbon isotope signals, but, as in Neoproterozoic carbonates, tests to demonstrate their immunity to late diagenetic alterations are always recommended.

In the region where the Itamaracá drill hole is located, the Paraíba Basin received the least continental influence as an open marine environment. The sites of the Poty and Olinda drill holes were subject to a relatively higher inflow of continental sediments (Fig. 3; Tables 1–3). Therefore, none of the drill holes are located in a restricted environment implying high evaporation; this is clear from the behaviour of the REE results (e.g. Ce) in the Poty Quarry drill hole, which was actually a near-shore environment with episodic mixing of continental water and sediments.

In thin sections, limestones from the three drill holes show no sign of late diagenesis. Mn/Sr ratios are lower than 2 in *c.* 94% of the analysed samples, confirming little to no post-depositional diagenetic alteration, implying near-primary isotopic values.

Holser (1997) has associated the absence or weakly negative or positive Ce anomalies, anoxia and carbon isotope excursions to extinction events, including the KTB mass extinction. Carbonates that recorded the KTB in the Paraíba Basin have weak to absent negative Ce anomaly, carbon isotope excursions and register an anoxic event (the presence of pyrite nodules and a discrete negative Eu anomaly).

Conclusions

Based on the behaviour of REEs in carbonates around the KTB in the Paraíba Basin, we assume that $\delta^{13}C$ pathways can be used as a global correlation parameter. Absent to weakly positive Ce anomalies (−0.1–0.002) coincide with a decrease, followed by an increase, in $\delta^{13}C$ values (from 2.3 to 1.8‰, and back to 2.3‰) and an increase in mercury values (from 0.4 to 2.7 ng g^{-1}).

Mercury, being a volatile element, probably spread into the atmosphere during the intense volcanism of the Deccan in India and was deposited all over the surface of the Earth. In two of the three drill holes, total mercury increases immediately after the KTB and, in two of them, mercury spikes (four of them in one case) precede this transition, providing evidence of volcanic activity/meteorite impacts predating the transition. Mercury shows a stratigraphic variation coincident with $\delta^{13}C$ and $\delta^{18}O$ stratigraphies across the KTB. The subtle increase in mercury content exactly across this transition seems to be compatible with coeval volcanism. This contention seems to support that large concomitant volcanism (either local or of global influence) has been responsible, at least in part, for the drastic climatic environmental changes in the Cretaceous–Palaeogene transition.

We thank Gilsa M. Santana and Vilma S. Bezerra for assistance with stable isotope analyses in the LABISE. MVNS is grateful to the National Council for Scientific and Technological Development (CNPq) for a scholarship during graduate studies at the Federal University of Pernambuco. This study was supported by the Paraíba Drilling Project/UFPE/CNPq/Princeton University and by grants to ANS (CNPq 470399/2008 and FACEPE APQ 0727-1.07/08). This is the contribution no. 258 of the NEG-LABISE.

References

Albertão, G. A. 1993. *Abordagem Interdisciplinar e Epistemológica sobre as Evidências do Limite Cretáceo-Terciário, com Base em Leituras Efetuadas no Registro Sedimentar das Bacias da Costa Leste Brasileira*. Dissertação de Mestrado, Departamento de Geologia da Escola de Minas da Universidade Federal de Ouro Preto.

Albertão, G. A., Koutsoukos, E. A. M., Regali, M. P. S., Attrep, M. Jr. & Martins, P. P., Jr. 1994. The Cretaceous–Tertiary boundary in southern low-latitude regions: preliminary study in Pernambuco, northeastern Brazil. *Terra Nova*, **6**, 366–375.

Albertão, G. A. & Martins, P. P., Jr. 1996. A possible tsunami deposit at the cretaceoustertiary boundary in Pernambuco, northeastern Brazil. *Sedimentary Geology*, **104**, 189–201.

Almeida, F. F. M., Carneiro, C. D. R. & Mizusaki, A. M. P. 1996. Correlação do magmatismo das bacias da margem continental brasileira com o das áreas emersas adjacentes. *Revista Brasileira de Geociências*, **26**, 125–138.

Alvarez, L. W., Alvarez, W., Asaro, F. & Michael, H. V. 1980. Extraterrestrial cause for the Cretaceous–Tertiary extinction. *Science*, **208**, 1095–1108.

Archibald, J. D. & 28 Additional Authors. 2010. Cretaceous extinctions: multiple causes. *Science*, **328**, 973–976.

Banner, J. L., Hanson, G. N. & Meyers, W. J. 1988. Rare earth element and Nd isotopic variations in regionally extensive dolomites from the Burlington–Keokuk Formation (Mississippian): implications for REE mobility during carbonate diagenesis. *Journal of Sedimentary Petrology*, **58**, 415–432.

Barbosa, J. A. 2007. *A deposição carbonática na faixa costeira Recife–Natal: aspectos estratigráficos, geoquímicos e paleontológicos*. Doctoral dissertation, Federal University of Pernambuco.

Barbosa, J. A., Souza, E. M., Lima Filho, M. F. & Neumann, V. H. 2003. A estratigrafia da Bacia Paraíba: uma reconsideração. *Estudos Geológicos*, **13**, 89–108.

Barbosa, J. A., Viana, M. S. S. & Neumann, V. H. 2006. Paleoambientes e icnofácies da seqüência carbonática (Cretáceo e Paleogeno) da Bacia da Paraíba, NE do Brasil. *Revista Brasileira de Geociências*, **36**, 73–90.

Beerling, D. J., Harfoot, M., Lomax, B. & Pyle, J. 2007. The stability of the stratospheric ozone layer during the end-Permian eruption of the Siberian Traps. *Philosophical Transactions of the Royal Society*, **365**, 1843–1866.

Berner, A. R. 2002. Examination of hypotheses for the Permo–Triassic boundary extinction by carbon cycle modeling. *Proceedings of the National Academy of Science USA*, **99**, 4172–4177.

Beurlen, K. 1967*a*. Estratigrafia da faixa sedimentar costeira Recife–João Pessoa. *São Paulo, Boletim de Geologia*, **16**, 43–53.

Beurlen, K. 1967*b*. Paleontologia da faixa sedimentar costeira Recife–João Pessoa. *São Paulo, Boletim de Geologia*, **16**, 73–79.

Bohor, B. F. 1990. Shocked quartz and more: impact signatures in Cretaceous/Tertiary boundary clays. *In*: Sharpton, V. L. & Ward, P. D. (eds) *Global Catastrophes in Earth History: An Interdisciplinary Conference on Impacts, Volcanism, and Mass Mortality*.

Geological Society of America, Special Papers, **247**, 335–342.

Bohor, B. F., Modreski, P. J. & Foord, E. E. 1984. Shocked quartz in the Cretaceous–Tertiary boundary clays: evidence for a global distribution. *Science*, **224**, 705–709.

Campbell, I. H., Czamanske, G. K., Fedorenko, V. A., Hill, R. I. & Stepanov, V. 1992. Synchronism of the Siberian Traps and the Permian–Triassic Boundary. *Science*, **258**, 1760–1763.

Chatterjee, S. & Rudra, D. K. 1996. KT events in India: impact, volcanism and dinosaur extinction. *Memoirs of the Queensland Museum*, **39**, 489–532.

Chatterjee, S., Guven, N., Yoshinobu, A. & Donofrio, R. 2003. The Shiva Crater: implications for Deccan volcanism, Índia–Seychelles rifting, dinosaur extinction, and petroleum entrapment at the K–T boundary. *Geological Society of America Abstracts*, **35**, 168.

Claeys, P., Kiessling, W. & Alvarez, W. 2002. Distribution of Chicxulub ejecta at the Cretaceous–Tertiary boundary. *In*: Koeberl, C. & MacLeod, K. G. (eds) *Catastrophic Events and Mass Extinctions: Impacts and Beyond*. Geological Society of America, Special Papers, **356**, 55–68.

Courtillot, V. 1999. *Evolutionary Catastrophes: The Science of Mass Extinction*. Cambridge University Press, Cambridge.

Craig, H. 1957. Isotopic standards of carbon and oxygen and correction factors for mass-spectrometric analysis of carbon dioxide. *Geochimica et Cosmochimica Acta*, **12**, 133–149.

Elderfield, H. & Graves, M. 1982. The rare earth elements in seawater. *Nature*, **296**, 214–219.

Ferrara, F., Mazzolai, B., Lanzillotta, E., Nucaro, E. & Pirrone, N. 2000. Volcanoes as emission sources of atmospheric mercury in the Mediterranean Basin. *The Science of the Total Environment*, **259**, 115–121.

Fleet, A. J. 1984. Aqueous and sedimentary geochemistry of the rare earth elements. *In*: Henderson, P. (ed.) *Developments in Geochemistry*. *Rare Earth Elements Geochemistry*. British Museum, London, 343–373.

Frimmel, E. H. 2009. Trace element distribution in Neoproterozoic carbonates as palaeoenvironmental indicator. *Chemical Geology*, **258**, 338–353.

Frimmel, E. H. 2010. On the reliability of stable carbon isotopes for Neoproterozoic chemostratigraphic correlation. *Precambrian Research*, **182**, 239–253.

Goldberg, E. D. 1961. Chemistry in the oceans. *In*: *Oceanography*. American Association for the Advancement of Science, Washington, DC, 583–597.

Haskin, L. A., Wildeman, T. R. & Haskin, M. A. 1968. An accurate procedure for the determination of the rare earths by neutron activation. *Journal of Radioanalytical Chemistry*, **1**, 337–348.

Hoffman, C., Feraud, G. & Courtillot, V. 2000. $^{40}Ar/^{39}Ar$ dating of mineral separates and whole rocks from the Western Ghats lava pile: further constraints on duration and age of Deccan traps. *Earth and Planetary Science Letters*, **180**, 13–27.

Hogdahl, O. T., Melsom, S. & Bowen, V. T. 1968. Neutron activation of lanthanide elements in seawater. *Advances in Chemistry Series*, **73**, 308–325.

Holser, W. 1997. Evaluation of the application of rare-earth elements to paleoceanography. *Palaeogeography, Palaeoclimatology, Palaeoecology*, **132**, 309–323.

Jiedong, Y., Weiguo, S., Zongzhe, W., Yaosong, X. & Xiancong, T. 1999. Variations in Sr and C isotopes and Ce anomalies in successions from China: evidence for the oxygenation of Neoproterozoic seawater? *Precambrian Research*, **93**, 215–233.

Kegel, W. 1955. *Geologia do fosfato de Pernambuco. Divisão de Geologia e Mineralogia,* Departamento Nacional da Produção Mineral, Rio de Janeiro, **157**.

Keller, G. 2001. The end-Cretaceous mass extinction in the marine realm: year 2000 assessment. *Planetary and Space Science*, **49**, 817–830.

Keller, G. 2005. Impacts, volcanism and mass extinction: random coincidence or cause and effect? *Australian Journal of Earth Science*, **52**, 725–757.

Keller, G., Stinnesbeck, W., Adatte, T. & Stüben, D. 2003. Multiple impacts across the Cretaceous–Tertiary boundary. *Earth-Science Reviews*, **62**, 327–363.

Kelley, P. S. & Gurov, E. 2002. Boltysh, another end Cretaceous impact. *Meteoritics & Planetary Science*, **37**, 1031–1043.

Knesel, K. M., Souza, Z. S., Vasconcelos, P. M., Cohen, B. E. & Silveira, F. V. 2011. Young volcanism in the Borborema Province, NE Brazil, shows no evidence for a trace of the Fernando de Noronha plume on the continent. *Earth and Planetary Science Letters*, **302**, 38–50.

Kot, F. S., Green-Ruiz, C., Páez-Osuna, F., Shumilin, E. N. & Rodríguez-Meza, D. 1999. Distribution of mercury in sediments from La Paz Lagoon, Peninsula of Baja California, Mexico. *Bulletin Environmental Contamination Toxicology*, **63**, 45–51.

Koutsoukos, E. A. M. 1998. An extraterrestrial impact in the early Danian: a secondary K/T boundary event? *Terra Nova*, **10**, 68–73.

Lacerda, L. D. & Marins, R. V. 2006. Geoquímica de sedimentos e o monitoramento de metais na plataformal continental do Nordeste Oriental do Brasil. *Geochimica Brasiliensis*, **20**, 123–135.

Liu, Y. G., Miah, M. R. U. & Schmitt, R. A. 1988. Cerium: a chemical tracer for paleo-oceanic redox conditions. *Geochimica et Cosmochimica Acta*, **52**, 1361–1371.

Mabesoone, J. M. 1991. Sedimentos do Grupo Paraíba: Revisão geológica da faixa sedimentar costeira de Pernambuco, Paraíba, e parte do Rio Grande do Norte. *Boletim Estudos e Pesquisa Série B*, **10**, 63–71.

Mabesoone, J. M. & Alheiros, M. M. 1988. Origem da bacia sedimentar costeira Pernambuco-Paraíba. *Revista Brasileira de Geociências*, **18**, 476–482.

Mabesoone, J. M. & Alheiros, M. M. 1991. Base Estrutural – Faixa sedimentar costeira de Pernambuco, Paraíba e parte do Rio Grande do Norte. *In*: Mabesoone, J. M. (ed.) Revisão geológica da faixa sedimentar costeira de Pernambuco, Paraíba e parte do Rio Grande do Norte. *Estudos Geológicos*, **10**, 33–43.

Mabesoone, J. M. & Alheiros, M. M. 1993. Evolution of the Pernambuco-Paraíba-Rio Grande do Norte Basin and the problem of the South Atlantic connection. *Geologie en Mijnbouw*, **71**, 351–362.

MARINS, R. V., PAULA FILHO, F. J., MAIA, S. R. R., LACERDA, L. D. & MARQUES, W. S. 2004. Distribuição de mercúrio total como indicador de poluição urbana e industrial na costa Brasileira. *Química Nova*, **27**, 763–770.

MARTIN, J. M., HOGDAHL, O. & PHILPOTT, A. 1976. Rare earth element supply for the ocean. *Journal of Geophysical Research*, **81**, 3119–3124.

MARTINEZ-RUIZ, F., ORTEGA-HUERTAS, M. & PALOMO, I. 1999. Positive Eu anomaly development during diagenesis of the K/T boundary ejecta layer in the Agost section (SE Spain): implications for trace-element remobilization. *Terra Nova*, **11**, 290–296.

MARTINEZ-RUIZ, F., ORTEGA-HUERTAS, M. & RIVAS, P. 2006. Rare earth element composition as evidence of the precursor material of Cretaceous–Tertiary boundary sediments at distal sections. *Chemical Geology*, **232**, 1–11.

MCCREA, J. M. 1950. On the isotopic chemistry of carbonates and a paleotemperature scale. *Journal of Physical Chemistry*, **18**, 849–857.

MCLEAN, D. M. 1978. A terminal Mesozoic 'greenhouse': lessons from the past. *Science*, **201**, 401–406.

MCLEAN, D. M. 1991. Impact winter in the global K/T extinctions: no definitive evidences. *In*: LEVINE, J. S. (ed.) *Global Biomass Burning: Atmospheric, Climatic, and Biospheric Implications*. MIT Press, Cambridge, MA, Ch. 6, 493–508.

MCLENNAN, S. C. 1989. Rare earth in sedimentary rocks: influence of provenance and sedimentary processes. *In*: LIPIN, B. R. & MCKAY, G. A. (eds) RIBBE, P. H. (series ed.) *Reviews in Mineralogy, Geochemistry and Mineralogy of Rare Earth Element*. Mineralogical Society of America, Washington, DC, **21**, 169–225.

MENOR, E. A. 1975. *La sedimentation phosphate. Pétrographie, mineralogie et géochimie des gisements de Taíba (Senegal) et d'Olinda (Brésil)*. PhD thesis, Université Louis Pasteur, Strasbourg.

MENOR, E. A., SIAL, A. N., FERREIRA, V. P. & BOUJO, A. 1999. Carbon- and oxygen-isotopic behavior of carbonate rocks of the phosphatic Gramame Formation, Pernambuco–Paraíba coastal basin, northeastern Brazil. *International Geology Review*, **41**, 593–606.

MICHARD, A., ALBARÈDE, F., MICHARD, G., MINSTER, J. F. & CHARLOU, J. L. 1983. Rare earth elements and uranium in high temperature solutions from the East Pacific Rise hydrothermal vent fields (13°N). *Nature*, **303**, 795–797.

MORGAN, J. V., LANA, C. *ET AL*. 2006. Analyses of shocked quartz at the global K–P boundary indicate an origin from a single, high-angle, oblique impact at Chicxulub. *Earth and Planetary Science Letters*, **251**, 264–279.

NASCIMENTO-SILVA, M. V., SIAL, A. N., FERREIRA, V. P., NEUMANN, V. H. M., BARBOSA, A., PIMENTEL, M. M. & LACERDA, L. D. 2011. Cretaceous–Paleogene transition at the Paraíba Basin, northeastern Brazil: carbon-isotope and mercury subsurface stratigraphies. *Journal of South American Earth Sciences*, **32**, 379–392, http://dx.doi.org/10.1016/j.jsames.2011.02.014.

NEUMANN, V. H., BARBOSA, J. A., NASCIMENTO-SILVA, M. V., SIAL, A. N. & LIMA-FILHO, M. L. 2009. Sedimentary development and isotope analysis of deposits at the Cretaceous/Paleogene transition in the Paraiba Basin, NE Brazil. *Geologos*, **15**, 103–113.

NOTHDURFT, L. D., WEBB, G. E. & KAMBER, B. S. 2004. Rare earth element geochemistry of Late Devonian reefal carbonates, Canning Basin, Western Australia: confirmation of a seawater REE proxy in ancient limestones. *Geochimica et Cosmochimica Acta*, **68**, 263–283.

PIPER, D. Z. 1974. Rare earth elements in the sedimentary cycle: summary. *Chemical Geology*, **14**, 285–304.

RENNE, P. R., BLACK, M. T., ZICHAO, Z., RICHARDS, M. A. & BASU, A. R. 1995. Synchrony and causal relations between Permian–Triassic boundary crises and Siberian flood volcanism. *Science*, **269**, 1413–1416.

ROOS-BARRACLOUGH, F., MARTINEZ-CORTIZAS, A., GARCIA-RODEJA, E. & SHOTYK, W. 2002. A 14500 year record of the accumulation of atmospheric mercury in peat: volcanic signals, anthropogenic influences and a correlation to bromine accumulation. *Earth Planetary Science Letters*, **202**, 435–451.

ROYER, D. L., BERNER, R. A., MONTAÑEZ, I. P., TABOR, N. J. & BEERLING, D. J. 2004. CO_2 as a primary driver of Phanerozoic climate. *Geological Society of America Today*, **14**, 4–10.

SCHULTZE, P. *ET AL*. 2010. The Chicxulub Asteroid impact and mass extinction at the Cretaceous–Paleogene boundary. *Science*, **327**, 1214–1218.

SHETH, H. C. 2005. Were the Deccan flood basalts derived in part from ancient oceanic crust within the Indian continental lithosphere? *Gondwana Research*, **8**, 109–127.

SHIMIZU, H. & MASUDA, A. 1977. Cerium in cherts as an indication of marine environment of its formation. *Nature*, **266**, 346–348.

SIAL, A. N., LONG, L., PESSOA, D. A. R. & KAWASHITA, K. 1981. Potassium–argon ages and strontium isotope geochemistry of Mesozoic and Tertiary basaltic rocks, northeastern Brazil. *Academia Brasileira de Ciências*, **53**, 115–121.

SIAL, A. N., GAUCHER, C. *ET AL*. 2010. C-, Sr-isotope and Hg chemostratigraphy of Neoproterozoic cap carbonates of the Sergipano Belt, northeastern Brazil. *Precambrian Research*, **182**, 351–372.

SMIT, J. 1999. The global stratigraphy of the Cretaceous–Tertiary boundary impact ejecta. *Annual Review of Earth and Planetary Sciences*, **27**, 75–113.

SMIT, J. & KLAVER, G. 1981. Sanidine spherules at the Cretaceous–Tertiary boundary indicate a large impact event. *Nature*, **292**, 47–49.

SOUZA, E. M. 1998. *Levantamento radiométrico das unidades estratigráficas da Bacia Paraíba*. Centro de Tecnologia e Geociências, Universidade Federal de Pernambuco, tese de mestrado.

SOUZA, E. M. 2006. *Estratigrafia da seqüência clástica inferior (andares Coniaciano–Maastrichtiano Inferior) da Bacia da Paraíba, e suas implicações paleogeográficas*. Doctoral dissertation, Federal University of Pernambuco.

STEWART, S. A. & ALLEN, J. P. 2002. A 20-km-diameter multi-ringed impact structure in the North Sea. *Nature*, **418**, 520–523.

STINNESBECK, W. & KELLER, G. 1996. Environmental changes across the Cretaceous–Tertiary boundary in Northeastern Brazil. *In*: MACLEOD, N. & KELLER, G. (eds) *Cretaceous–Tertiary Mass Extinctions: Biotic*

and Environmental Effects. Norton Press, New York, 451–470.

STINNESBECK, W., SCHULTE, P. *ET AL.* 2001. Late Maastrictian age of spherule deposits in the northeastern Mexico: implications for Chicxulub scenario. *Canadian Journal Earth Science*, **38**, 229–238.

TURNER, D. R. & WHITFIELD, M. 1979. Control of seawater composition. *Nature*, **281**, 468–469.

WESTPHAL, H. 2006. Limestone–marl alternations as environmental archives and the role of early diagenesis: a critical review. *International Journal of Earth Sciences*, **95**, 947–961.

WILDE, P., QUINBY-HUNT, M. S. & ERDTMANN, B. 1996. The whole-rock cerium anomaly: a potential indicator of eustatic sea-level changes in shales of the anoxic facies. *Sedimentary Geology*, **101**, 43–53.

WRIGHT, J., SCHRADER, H. & HOLSER, W. T. 1987. Paleoredox variations in ancient oceans recorded by rare earth elements in fossil apatite. *Geochimica et Cosmochimica Acta*, **51**, 637–634.